Electronic Supplementary Materials

Chirality Expression from Hierarchical Foldamer-Mesoscopic Helical Silica Frameworks

Piyanan Pranee,[a,c] Robin Hess,[a] Anthony Boudier,[a,b] Zakaria Anfar,[a] Matheus De Souza Lima Mendes,[a] Eric Merlet,[a] Wijak Yospanya,[c] Emilie Pouget,[a] Sylvain Nlate,[a] Céline Olivier,[b] Thierry Buffeteau,[b] Yann Ferrand*[a] and Reiko Oda*[a,c]

a. Institute of Chemistry & Biology of Membranes & Nano-objects (CBMN), University of Bordeaux, CNRS, Bordeaux INP, UMR 5248, F-33600 Pessac, France.

b. Institute of Molecular Sciences (ISM), University of Bordeaux, CNRS, Bordeaux INP, UMR 5255, F-33405 Talence, France.

c. WPI-Advanced Institute for Materials Research, Tohoku University, 2-1-1, Katahira, Aoba-Ku, Sendai 980-8577, Japan

Calculation

1. Dissymmetric factor (g_{abs} and g_{lum})

The dissymmetric factor (g_{abs}) was calculated by the equation:.

$$g_{abs} = \Delta\varepsilon/\varepsilon=\theta(mdeg)/(32980 \times A)$$

where θ is the ellipticity, A is the absorbance, ε is the molar extinction coefficient and Δ ε is the molar circular dichroism.

The dissymmetric factor (g_{lum}) was calculated by the equation:.

$$g_{lum} = CPL(mdeg).Ln(10)/(32980.F).$$

where F is the fluorescence at 505 nm.

2. Estimation of Q_4 volume.

Diameter	~ 20.31×10^{-8} cm
Height	~ 9.14×10^{-8} cm
Volume	2.96 x 10^{-21} cm^3/ Q_4 molecule

Therefore, Q_4 7.50 x 10^{-8} mole will contain volume as

$$= (7.50 \times 10^{-8}) \times 6.023 \times 10^{23} \times 2.96 \times 10^{-21} = 1.34 \times 10^{-4}\ cm^3$$

The equivalent quantity of Q_4 was calculated to be 7.5×10^{-8} mole which corresponds to 1.34×10^{-4} cm^3 when dried.

3. Calculation of the enantiomeric excess (ee%).

$$Fol_P \xrightarrow{k_1} Fol_M$$

$$Fol_P \xleftarrow[k_2]{} Fol_M$$

$$Fol_P = P - foldamers,\ Fol_M = M - foldamers,$$

$$-\frac{d[C_P]}{dt} = k_1[C_P] - k_2[C_M] \quad (1)$$

$$[C_P] = concentration\ of\ P - foldamers, [C_M] = concentration\ of\ M - foldamers$$

$$IF\ [C_{Fol}] = [C_P] + [C_M]$$

$$(2)\ [C_M] = [C_{Fol}] - [C_P]$$

$$[C_{Fol}] = Total\ concentration\ of\ foldamers$$

$$-\frac{d[C_P]}{dt} = k_1[C_P] - k_2([C_{Fol}] - [C_P])$$

$$-\frac{d[C_P]}{dt} = (k_1 + k_2)[C_P] - k_2[C_{Fol}]$$

$$(3)\ \frac{d[C_P]}{dt} + (k_1 + k_2)[C_P] = k_2[C_{Fol}]$$

$$IF\ equilibrium\ can\ reach\ racemic\ mixture: k_2 = k_1 = k$$

$$So\ (3)\ becomes: \frac{d[C_P]}{dt} + 2k[C_P] = k[C_{Fol}]$$

$$Solutions\ are: [C_P](t) = \alpha \cdot e^{-2kt} + \frac{[C_{Fol}]}{2}$$

$$\Delta A_{vis} = \Delta A_{PFol} + \Delta A_{MFol}$$

$$(4)\qquad \Delta A_{vis} = \Delta\varepsilon_{PFol} l[C_P](t) + \Delta\varepsilon_{MFol} l[C_M](t)$$

$$PFol\ and\ MFol\ being\ enantiomers: (5)\ \Delta\varepsilon_{PFol} = -\Delta\varepsilon_{MFol}$$

$$So\ (4)\ becomes\ using\ (5): \Delta A_{vis} = \Delta\varepsilon_{PFol} l([C_P](t) - [C_M](t))$$

$$Using\ (2): \Delta A_{vis} = \Delta\varepsilon_{RFol} l([C_P](t) - ([C_{Fol}] - [C_P](t)))$$

$$\Delta A_{vis} = \Delta\varepsilon_{RFol} l(2[C_P](t) - [C_{Fol}])$$

$$\Delta A_{vis} = \Delta\varepsilon_{PFol} l(2(\alpha \cdot e^{-2kt} + \frac{[C_{Fol}]}{2}) - [C_{Fol}])$$

$$\Delta A_{vis} = \Delta\varepsilon_{PFol} l 2\alpha \cdot e^{-2kt}$$

$$thus\ g_{abs}(t) = \frac{2\Delta\varepsilon_{PFol} l\alpha}{A_{tot}} \cdot e^{-2kt}$$

$$g_{abs}(t) = \Gamma \cdot e^{-2kt}$$

$$with\ \Gamma = \frac{2\Delta\varepsilon_{PFol} l\alpha}{A_{tot}}\ (this\ is\ a\ constant)$$

$$Here\ we\ can\ see\ that\ g_{abs}(t=0)\ =\ \Gamma$$

$$by\ continuity\ of\ the\ system\ g_{abs}(t=0)\ \approx\ \lim_{\delta t\to 0} g_{abs}(t=\ -\delta t)$$

$$which\ is\ the\ g_{abs}\ of\ the\ foldamers\ at\ the\ equilibrium\ inside\ the\ helice$$

LH-INHs

At 180 sec, 385 nm

$$g_{abs}(t) = \Gamma \cdot e^{-2(k)(t)}$$

$$g_{abs}(t) = \Gamma \cdot e^{-2(k)(180)}$$

$$-1.88 \times 10^{-4} = \Gamma \cdot e^{-360k} \quad \text{.....(1)}$$

At 300 sec, 385 nm

$$g_{abs}(t) = \Gamma \cdot e^{-2(k)(t)}$$

$$g_{abs}(t) = \Gamma \cdot e^{-2(k)(300)}$$

$$-1.11\ x\ 10^{-4} = \Gamma \cdot e^{-600k} \quad \text{.....(2)}$$

(1)/(2)

$$1.69 = e^{240k}$$

$$\mathbf{k = 2.19 \times 10^{-3}}$$

(1)

$$-1.88 \times 10^{-4} = \Gamma \cdot e^{-360k}$$

If $k = 2.19 \times 10^{-3}$

$$\mathbf{\Gamma = -4.13 \times 10^{-4}}$$

At 0 sec, 385 nm

$$g_{abs}(t) = \Gamma \cdot e^{-2(k)(0)}$$

$$g_{abs}(t) = \Gamma$$

$$\boldsymbol{g_{abs}(t) = -4.13 \times 10^{-4}}$$

g_{abs} of Chiral Q_8 (LH) = -1.0x10^{-2} (385 nm)

Therefore, ee% from (LH-INHs) ~4.1%

RH-INHs

At 180 sec, 385 nm

$$g_{abs}(t) = \Gamma \cdot e^{-2(k)(t)}$$

$$g_{abs}(t) = \Gamma \cdot e^{-2(k)(180)}$$

$$0.854 \times 10^{-4} = \Gamma \cdot e^{-360k} \quad \text{.....(1)}$$

At 300 sec, 385 nm

$$g_{abs}(t) = \Gamma \cdot e^{-2(k)(t)}$$

$$g_{abs}(t) = \Gamma \cdot e^{-2(k)(300)}$$

$$0.31\ x\ 10^{-4} = \Gamma \cdot e^{-600k} \quad \text{.....(2)}$$

(1)/(2)

$$2.75 = e^{240k}$$

$$\mathbf{k = 4.22 \times 10^{-3}}$$

(1)

$$0.854 \times 10 - 4 = \Gamma \cdot e^{-360k}$$

If $k = 4.22 \times 10^{-3}$

$$\mathbf{\Gamma = 3.90 \times 10^{-4}}$$

At 0 sec, 385 nm

$$g_{abs}(t) = \Gamma \cdot e^{-2(k)(0)}$$

$$g_{abs}(t) = \Gamma$$

$$\boldsymbol{g_{abs}(t) = 3.90 \times 10^{-4}}$$

g_{abs} of Chiral Q_8 (RH) = 1.0x10^{-2} (385 nm)

Therefore, ee% from (RH-INHs) ~3.9%

Supplementary Information

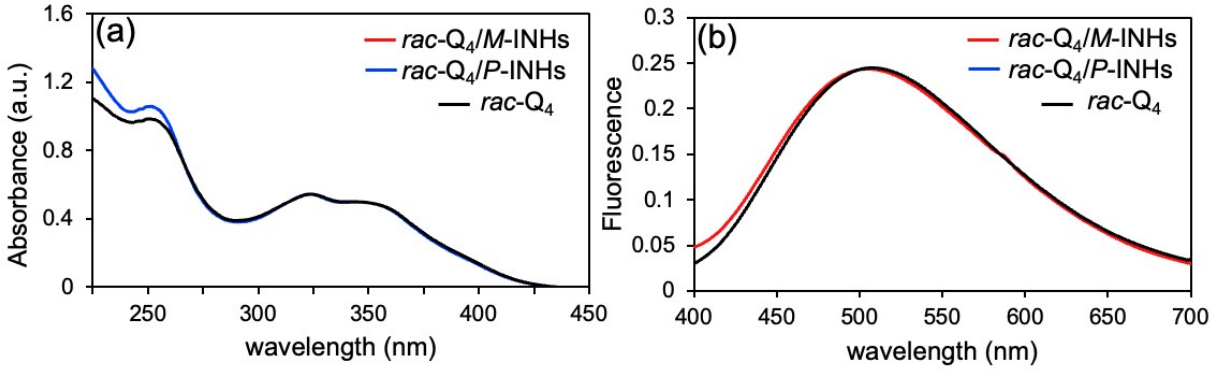

Figure S1. Absorption (a) and fluorescence (b) spectra of *rac*-Q_4, *rac*-Q_4/*M*-INHs, and *rac*-Q_4/*P*-INHs.

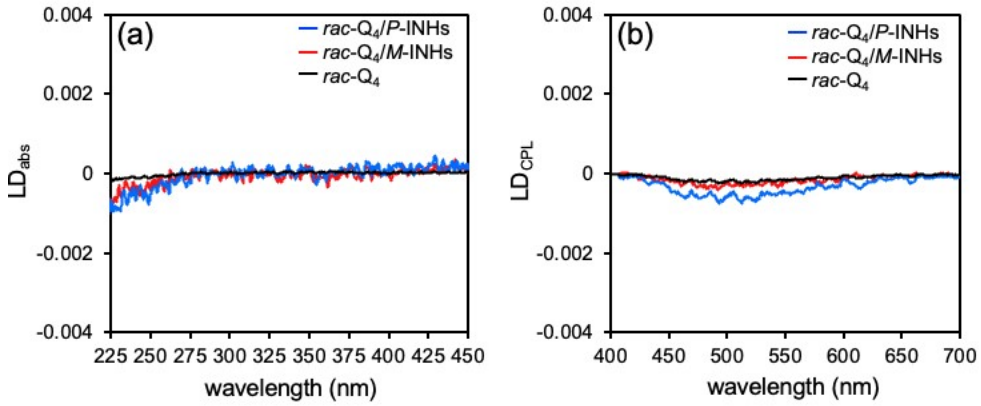

Figure S2. (a) LD_{abs} and (b) LD_{CPL} of *rac*-Q_4/*M*-INHs, *rac*-Q_4/*P*-INHs and *rac*-Q_4.

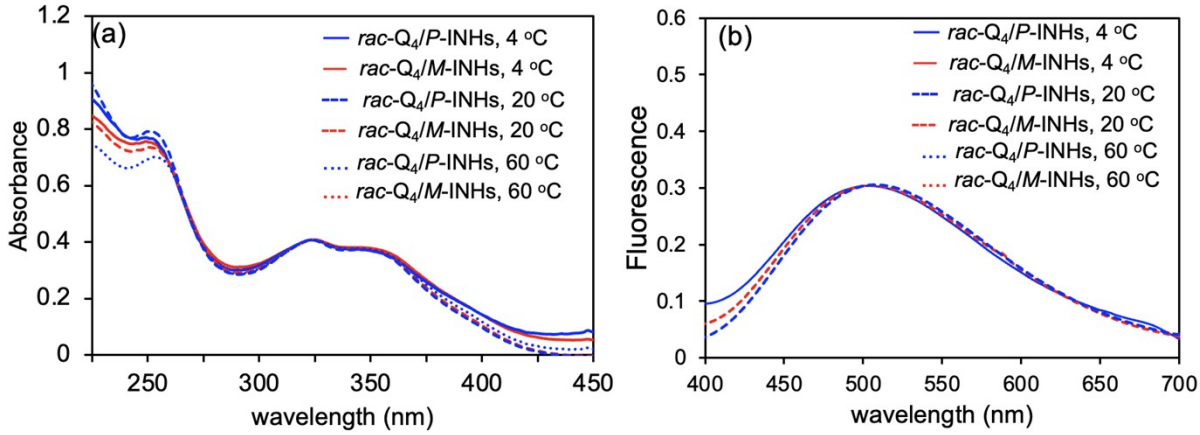

Figure S3. Absorption (a) and fluorescence (b) spectra of *rac*-Q_4/INHs after drop casting at 4 °C, 20 °C and 60 °C, (Q_4: 1 mM, 100 μL, INHs: 200 μg/2×2 cm^2).

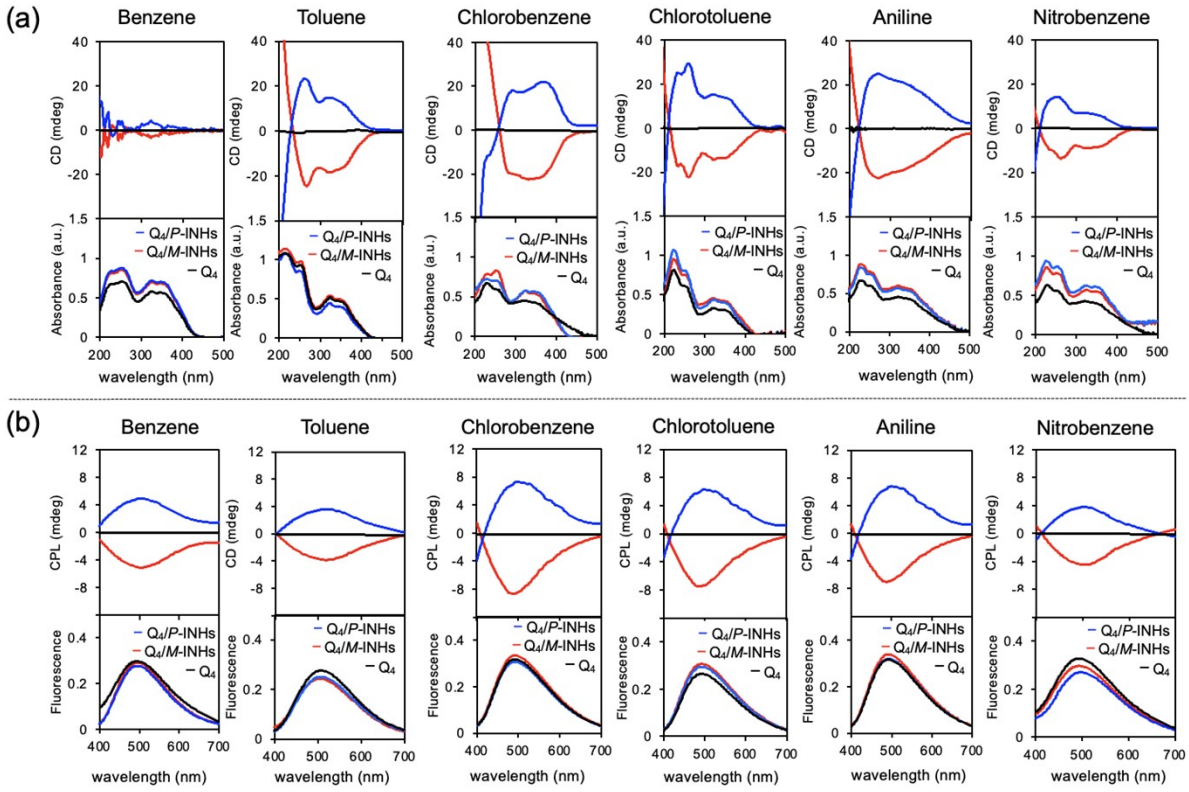

Figure S4. (a) ECD-absorption and CPL-fluorescence spectra of *rac*-Q_4/INHs and *rac*-Q_4 after drop-casting in different solvents, (*rac*-Q_4: 1 mM, 100 μL, INHs: 200 μg/2×2 cm^2).

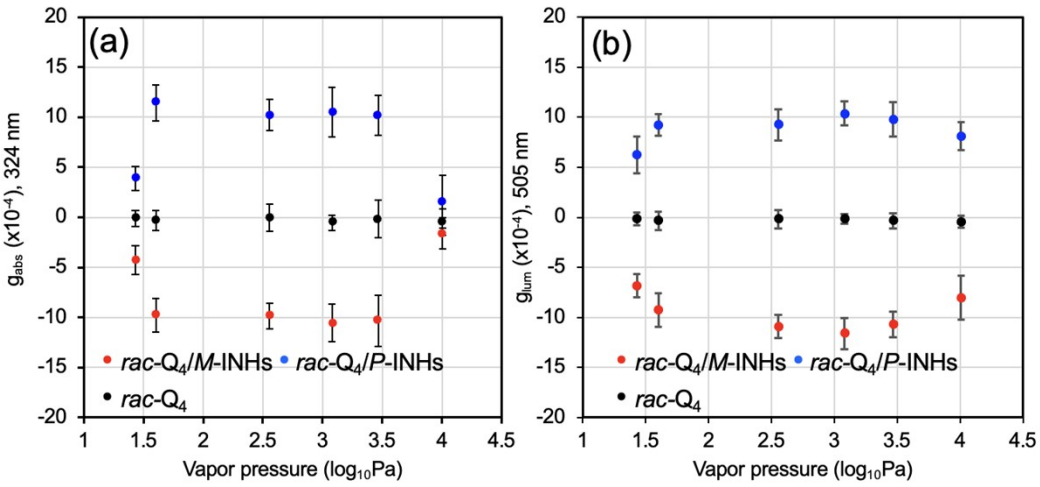

Figure S5. Plots between (a) g_{abs} and (b) g_{lum} versus vapor pressure (log_{10}Pa), (*rac*-Q_4: 1 mM, 100 μL, INHs: 200 μg/2×2 cm^2).

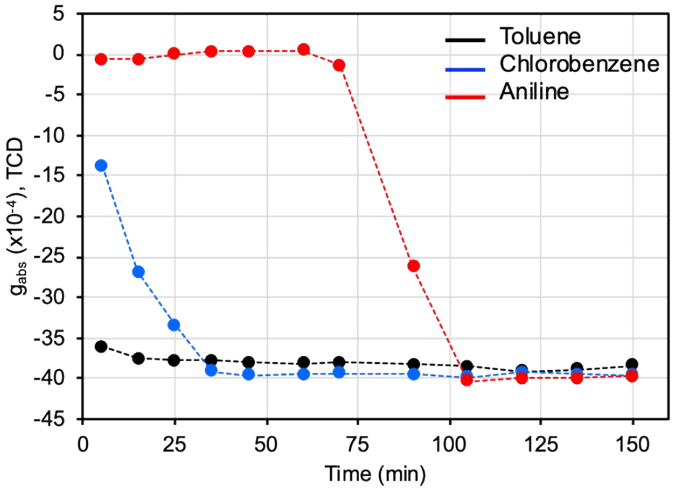

Figure S6. g_{abs} (at 324 nm) of *rac*-Q_4/INHs after drop-casting Q_4 in different solvents (toluene, chlorobenzene, aniline) during time (The CD response was detected from Transmission Circular Dichroism or TCD).

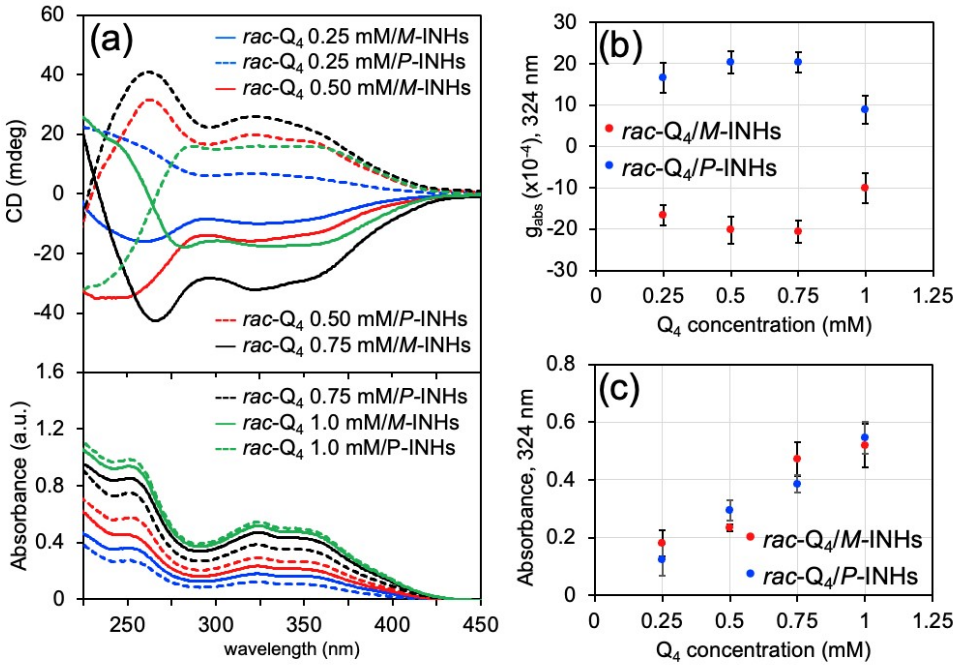

Figure S7. (a) ECD-absorption spectra, (b) g_{abs} and (c) absorbance at 324 nm of *rac*-Q_4/INHs by varying the concentration of *rac*-Q_4 (0.25-1.0 mM, 100 μL) on INHs (200 μg).

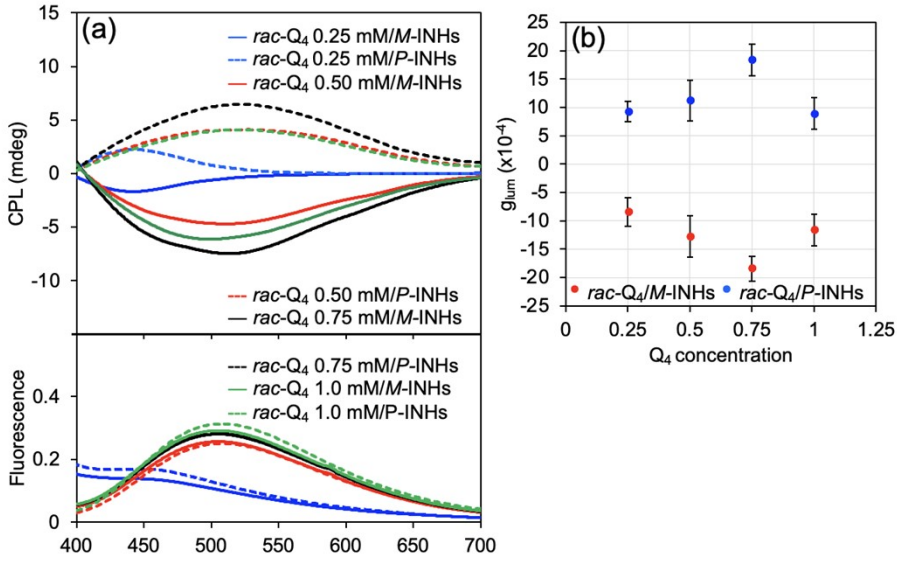

Figure S8. (a) CPL-fluorescence spectra and (b) g_{lum} of *rac*-Q_4/INHs by varying the concentration of Q_4 (0.25-1.0 mM, 100 μL) on INHs (200 μg), (λ_{ex} 320 nm).

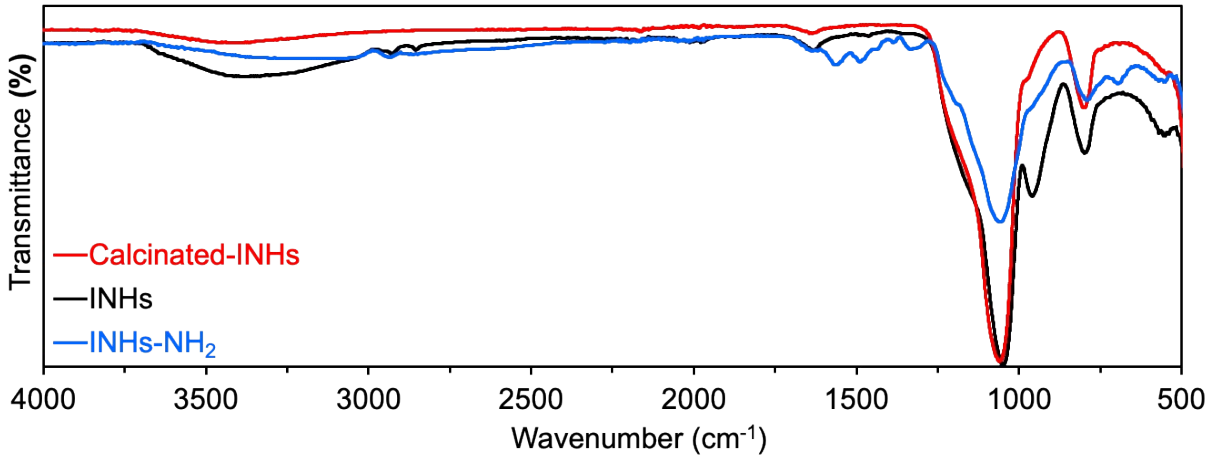

Figure S9. IR spectra of INHs, INHs-calcinated and INHs-NH_2

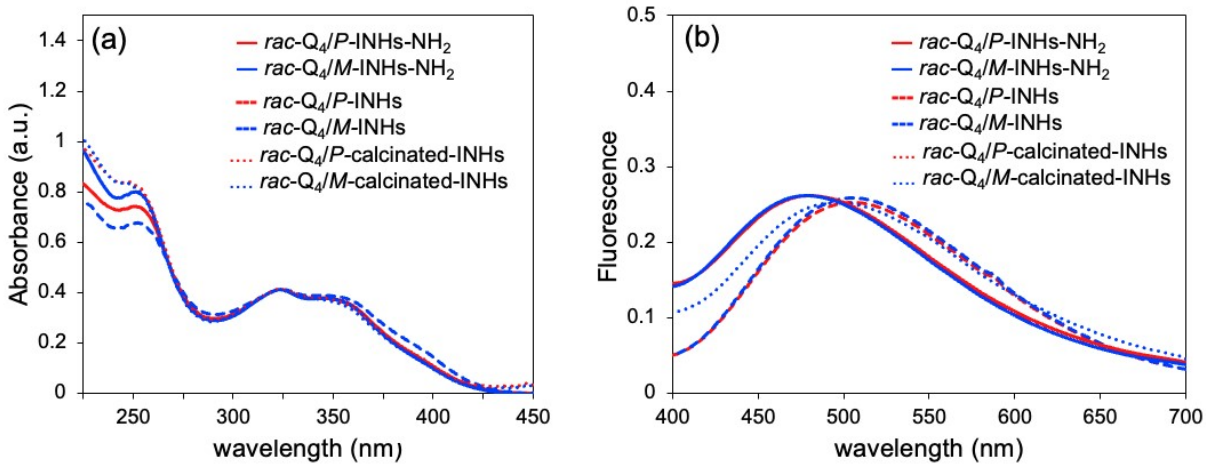

Figure S10. Absorption (a) and fluorescence (b) spectra of *rac*-Q_4/INHs, *rac*-Q_4/INHs-NH_2, *rac*-Q_4/calcinated-INHs, (λ_{ex} 320 nm).

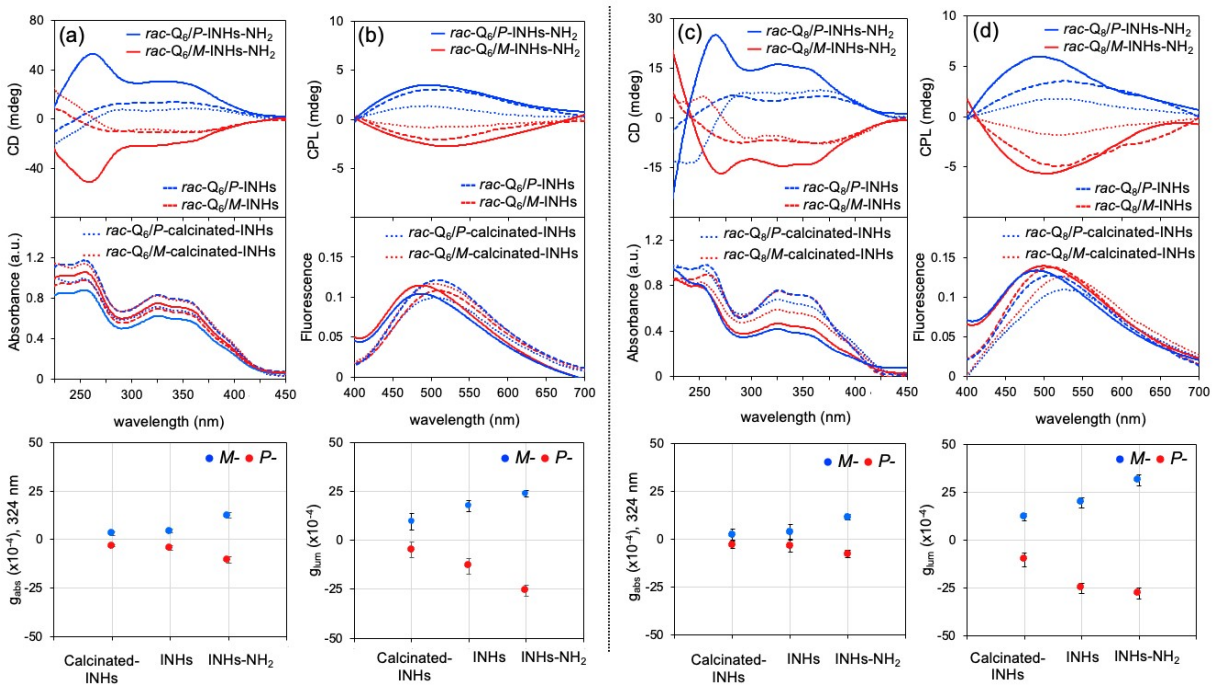

Figure S11. (a) ECD-absorption and (b) CPL-fluorescence spectra of *rac*-Q_6/INHs, *rac*-Q_6/INHs-NH_2 and *rac*-Q_6/calcinated-INHs, (λ_{ex} 320 nm). (c) ECD-absorption and (d) CPL-fluorescence spectra of *rac*-Q_8/INHs, *rac*-Q_8/INHs-NH_2 and *rac*-Q_8/calcinated-INHs, (λ_{ex} 320 nm).

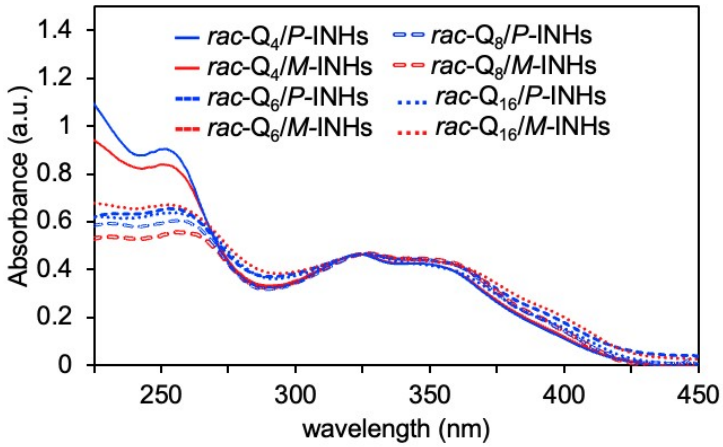

Figure S12. Absorption spectra of *rac*-Q_4/INHs, *rac*-Q_6/INHs, *rac*-Q_8/INHs and *rac*-Q_{16}/INHs.

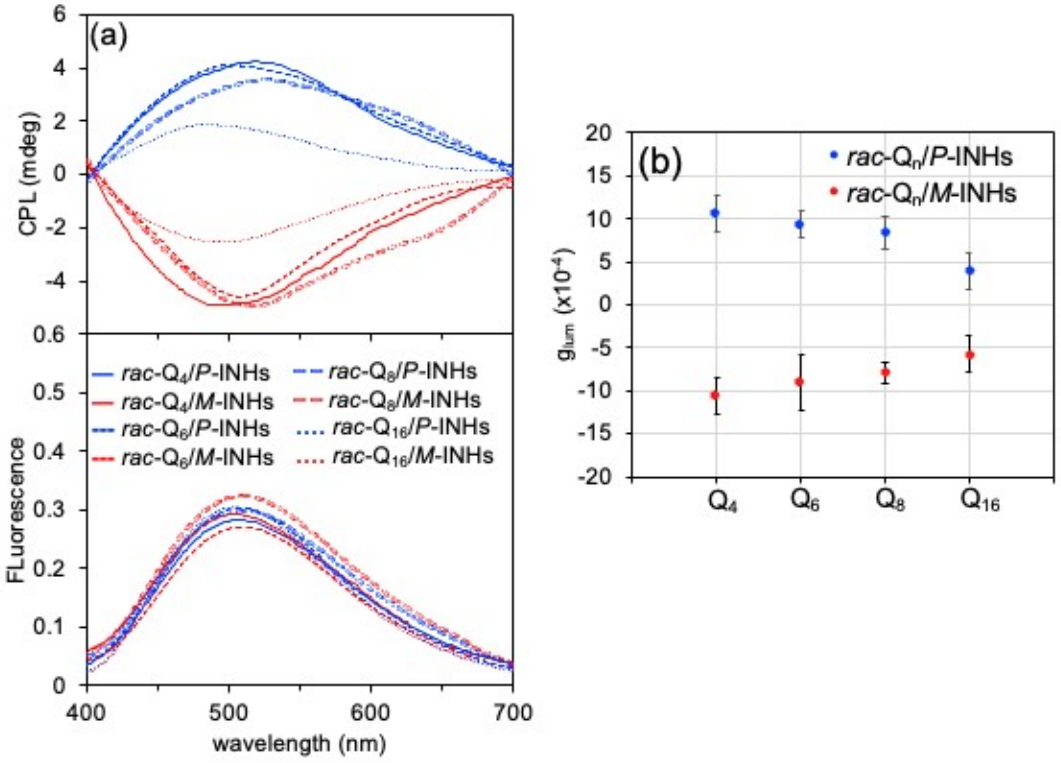

Figure S13. CPL-fluorescent spectra (a) and g_{lum} at 505 nm of *rac*-Q_4/INHs, *rac*-Q_6/INHs, *rac*-Q_8/INHs and *rac*-Q_{16}/INHs.

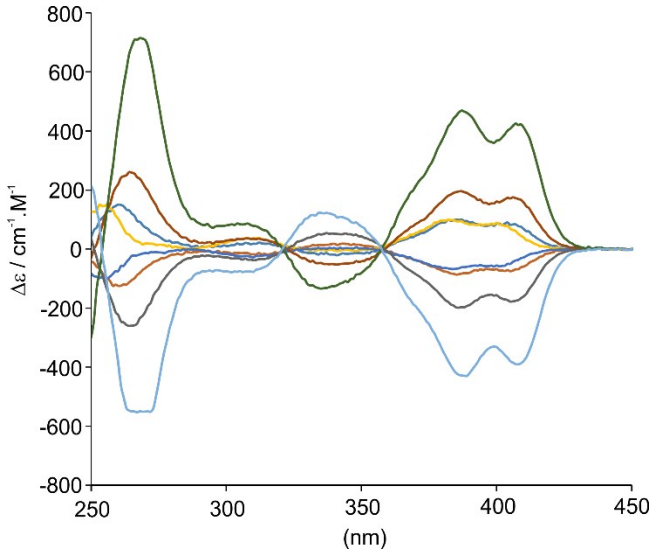

Figure S14. ECD spectra of *P*-Q_4 (yellow), *P*-Q_6 (blue), *P*-Q_8 (brown), *P*-Q_{16} (green) and their enantiomers *M*-Q_4 (blue), *M*-Q_6 (light brown), *M*-Q_8 (grey), *M*-Q_{16} (light blue).

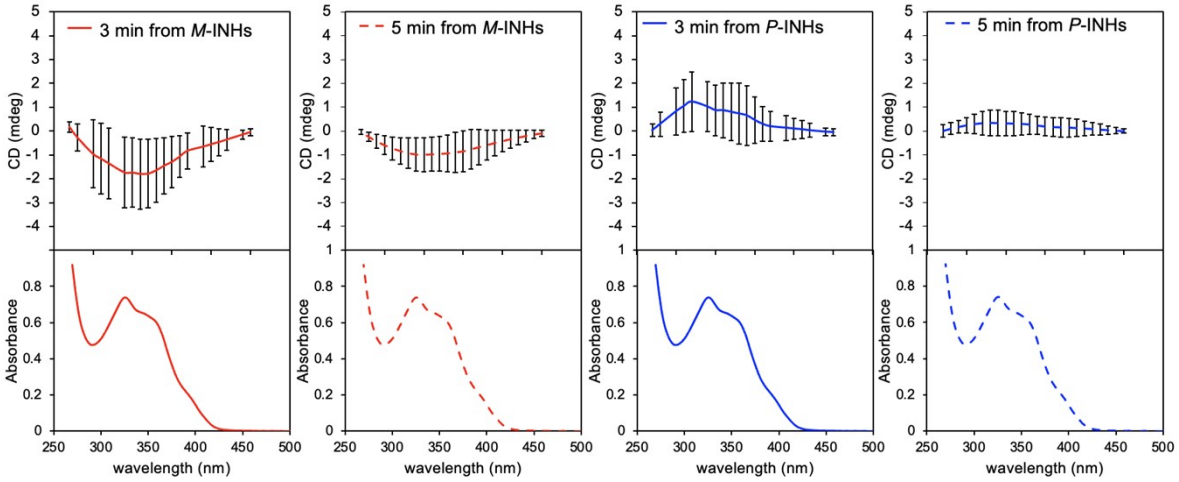

Figure S15. ECD-Absorption spectra of Q_8 at 3 and 5 min after washing out from *M*-/*P*-INHs (from 20-time experiment).

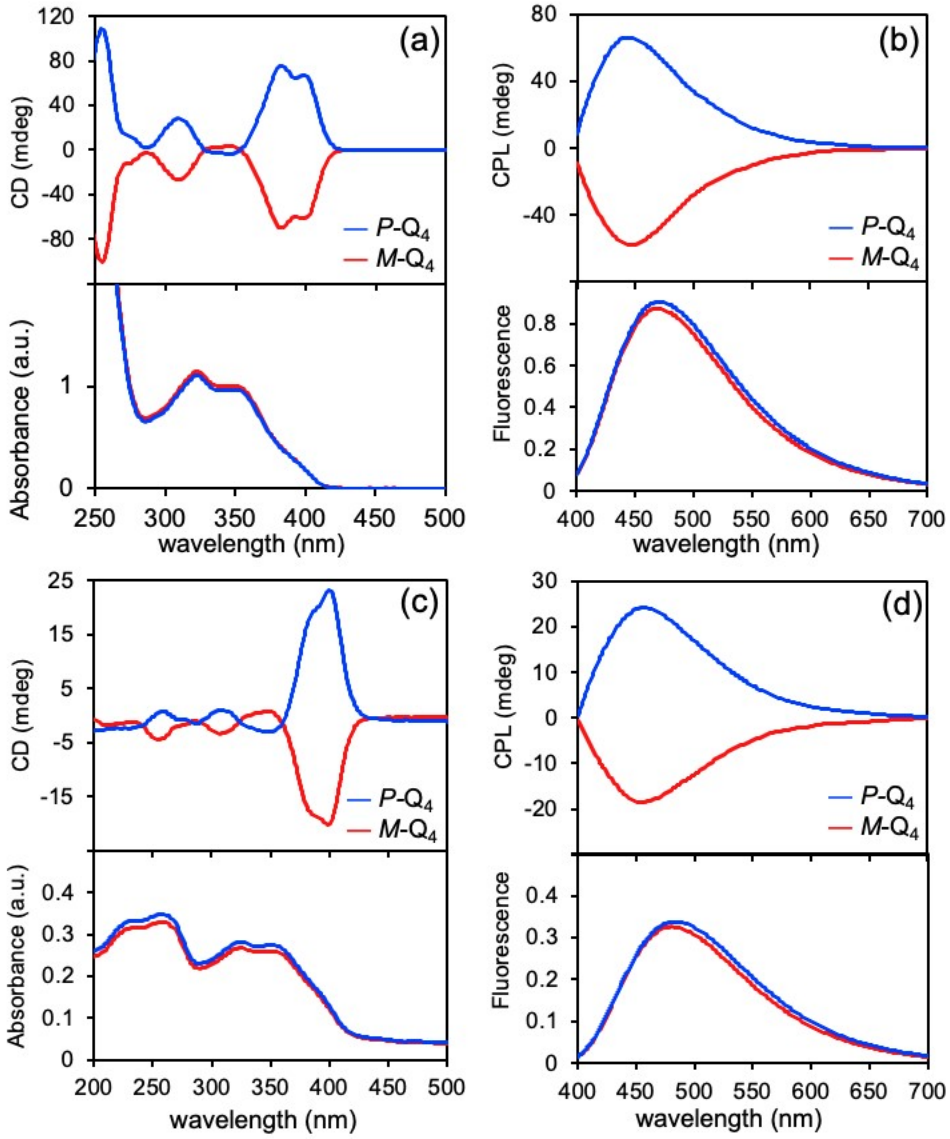

Figure S16. ECD-absorption and CPL-fluorescence spectra (λ_{ex} 320 nm) of *M*-Q_4 and *P*-Q_4 in $CHCl_3$ (a,b) and deposited onto a substrate (c, d).

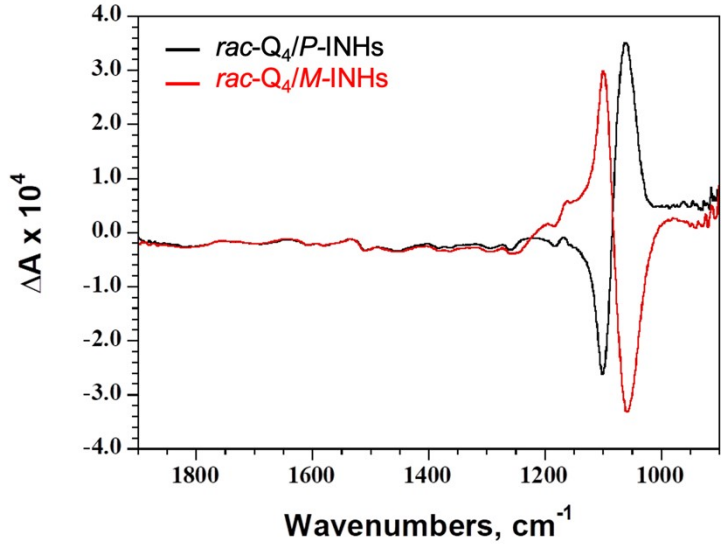

Figure S17. VCD spectra of *rac*-Q_4/*P*-INHs and *rac*-Q_4/*M*-INHs.

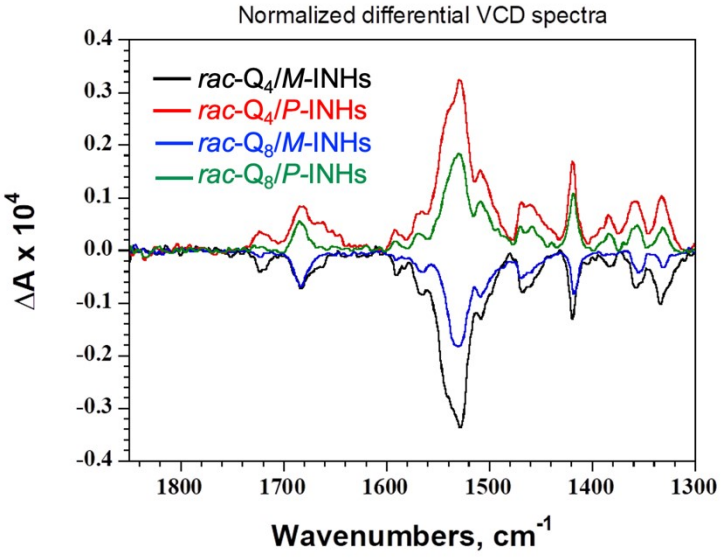

Figure S18. Differential (Q_n/*P*(*M*)-INHs - *P*(*M*)-INHs) VCD spectra of Q_4/INHs and Q_8/INHs normalized to the absorbance intensity of the 1540 cm^{-1} band, the most intense band of the foldamers.

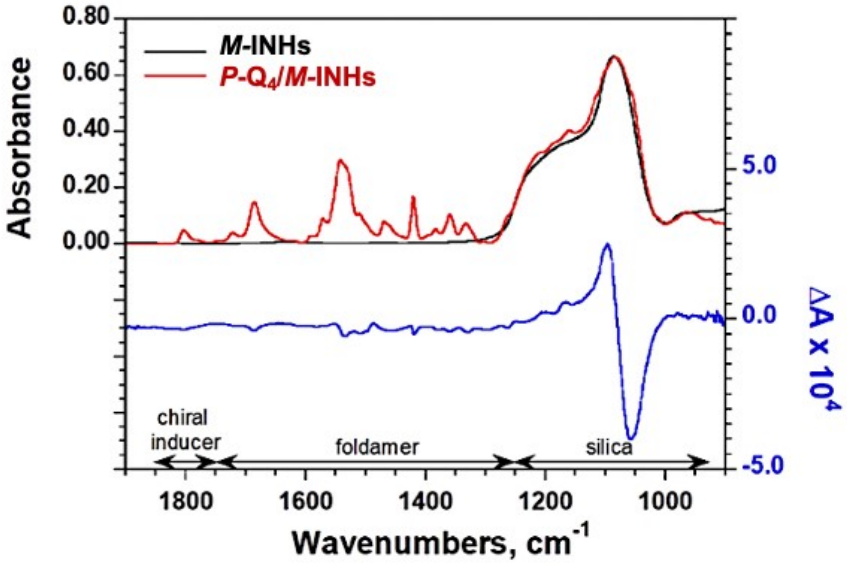

Figure S19. (top) IR spectra of *M*-INHs (black) and *P*-Q_4/*M*-INHs (red), (bottom) Raw VCD spectrum of *P*-Q_4/*M*-INHs (blue).

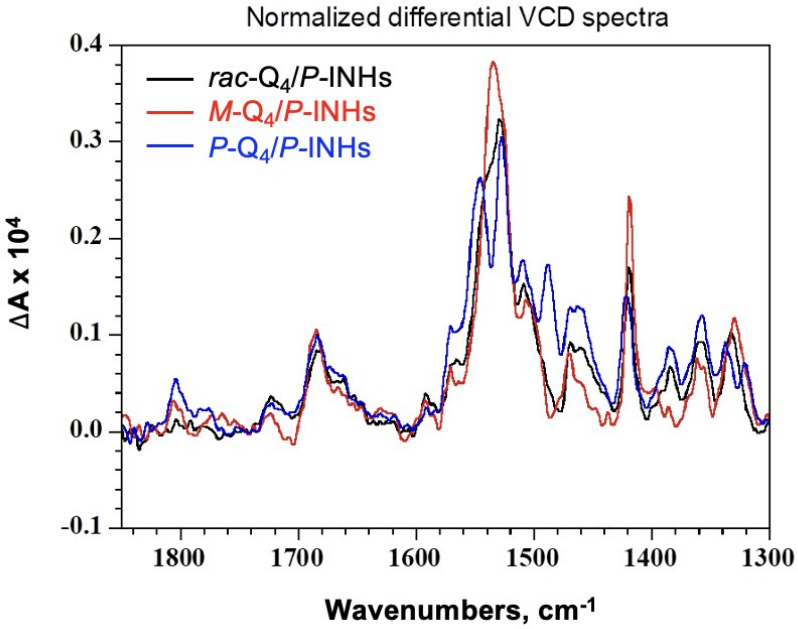

Figure S20. Normalized differential (*P*(*M*)-Q_4/*P*-INHs - *P*-INHs) VCD spectra of Q_4/*P*-INHs, *M*-Q_4/*P*-INHs, *P*-Q_4/*P*-INHs.

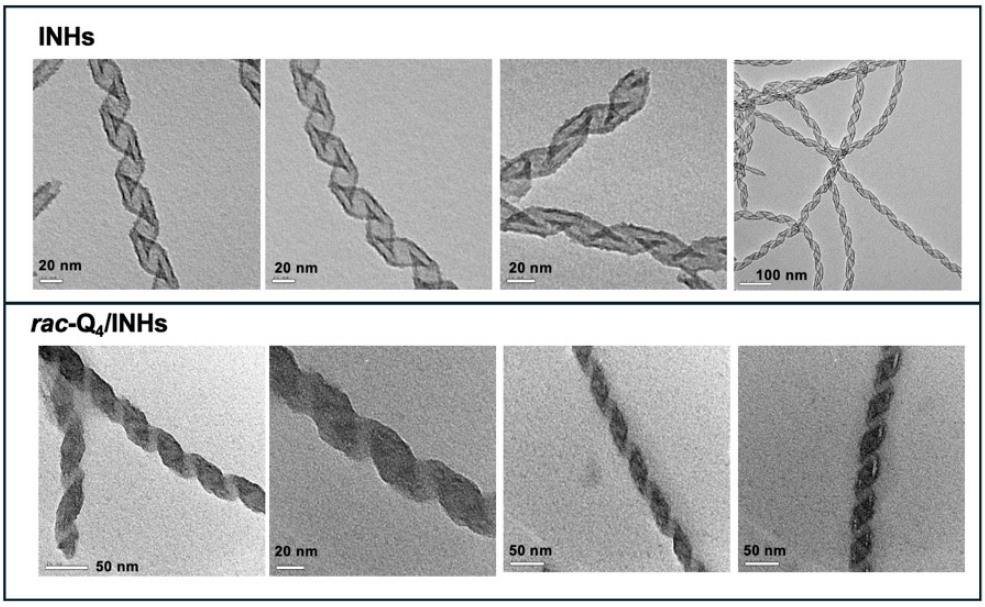

Figure S21 TEM images of drop cast INHs (top) and *rac-Q₄/INHs.*

Table S1. Solvents for drop-casting of *rac*-Q_4 foldamers

Solvent	Boiling point (°C)	Vapor pressure at 20 °C (Pa)
Benzene	80.3	10130
Toluene	110.8	2932
Chlorobenzene	132	1200
Chlorotoluene	157	359
Aniline	184.4	40
Nitrobenzene	211.1	27

Reference: MIDSIS-TROCS 4.0, Maritime Integrated Decision Support Information System on transport of Chemical Substance. (http://midsis.rempec.org)

Table S2. Infrared analysis: wavenumbers, assignment and origin of the major bands of *P*-Q_4

Wavenumber, cm^{-1}	Assignment	Origin
1802	υC=O	Ketone, camphanyl
1747	υC=O	COOMe
1720	υC=O	Amide 1, camphanyl
1686	υC=O	Amide 1, quinoline
1591, 1570	υC=C	quinoline

1540	δNH	Amide 2, quinoline
1511, 1469	υC=C	quinoline
1420	δCH_3	OiBu
1383, 1360, 1332	υC-C + δCH	quinoline
1265	υ_aC-O- φ	OiBu
1213	υ_aC-O- φ	OiBu
1160	υ_{ip}CH	quinoline
1116	υC-C + δC-C	quinoline
1055	υ_sC-O-φ	OiBu